Equatorial Spread *F* Simulations in the Peruvian Sector: Results and Diagnostics

Henrique C. Aveiro, David L. Hysell

Earth & Atmospheric Sciences
Cornell University

Motivation

Questions

- can we simulate CSI and gRT plasma instabilities?
- how well do ESF simulations compare to observations?
- which features are lost during observations?

Motivation

Questions

- can we simulate CSI and gRT plasma instabilities?
- how well do ESF simulations compare to observations?
- which features are lost during observations?

Study

- initial boundary value simulation in a realistic ionosphere using 3-D electrostatic potential solutions;
- remote diagnostics by ground-based airglow cameras and radars;
- *in situ* diagnostics by satellite-borne magnetometer.

Simulation Scheme

$$\nabla \cdot \mathbf{J} = 0 \rightarrow \nabla \cdot \left[\hat{\Sigma} \cdot \nabla \Phi\right] = \nabla \cdot \left[\hat{\Sigma} \cdot (\mathbf{E}_o + \mathbf{u} \times \mathbf{B}) + \hat{D} \cdot \nabla n + \hat{\Gamma} \cdot \mathbf{g}\right]$$

- finite differences – PDE numerical approximation of easy implementation;
- Biconjugate gradient stabilized method (BiCGStab) – iterative method suitable for the numerical solution of nonsymmetric linear systems.;

$$\begin{aligned} 0 &= n_\alpha q_\alpha (\mathbf{E} + \mathbf{V}_\alpha \times \mathbf{B}) \\ &\quad -\kappa_B T_\alpha \nabla n_\alpha \\ &\quad + n_\alpha m_\alpha [\mathbf{g} - \nu_{\alpha n}(\mathbf{V}_\alpha - \mathbf{U}) - \sum_{\beta \neq \alpha} \nu_{\alpha\beta}(\mathbf{V}_\alpha - \mathbf{V}_\beta)] \\ \frac{\partial n_\alpha}{\partial t} + \nabla \cdot (n_\alpha \mathbf{V}_\alpha) &= P_\alpha - L_\alpha \end{aligned}$$

- transport scheme $\rightarrow$ MUSCL – Monotone Upwind Scheme for Conservation Laws;
- Sweby ($\beta = 1.5$) flux limiter; and
- 2nd order Runge-Kutta integration.

Model inputs

- Temperature and Neutral Densities $\rightarrow$ NRL-MSISE-00;
- Electron Density $\rightarrow$ PIM – tuned slightly to account for day-to-day variability;
- Ion Composition $\rightarrow$ IRI-2007 – Atomic (O^+) and molecular (NO^+ and O_2^+) are included in the model, but light ions are not;
- Earth's Magnetic Field $\rightarrow$ IGRF;
- Neutral Winds $\rightarrow$ HWM-07;
- Background electric fields $\rightarrow$ JRO observations;
- independent Gaussian white noise was added to the initial number density with a 20% relative amplitude;
- coordinate system $\rightarrow$ magnetic dipole;
- simulation size: n_ϕ=189, $n_\perp$=159, $n_\parallel$=133. At the magnetic equator, Δ_ϕ=7 km, $\Delta_\perp$= 2.5 km.

Scanning radar diagnostic

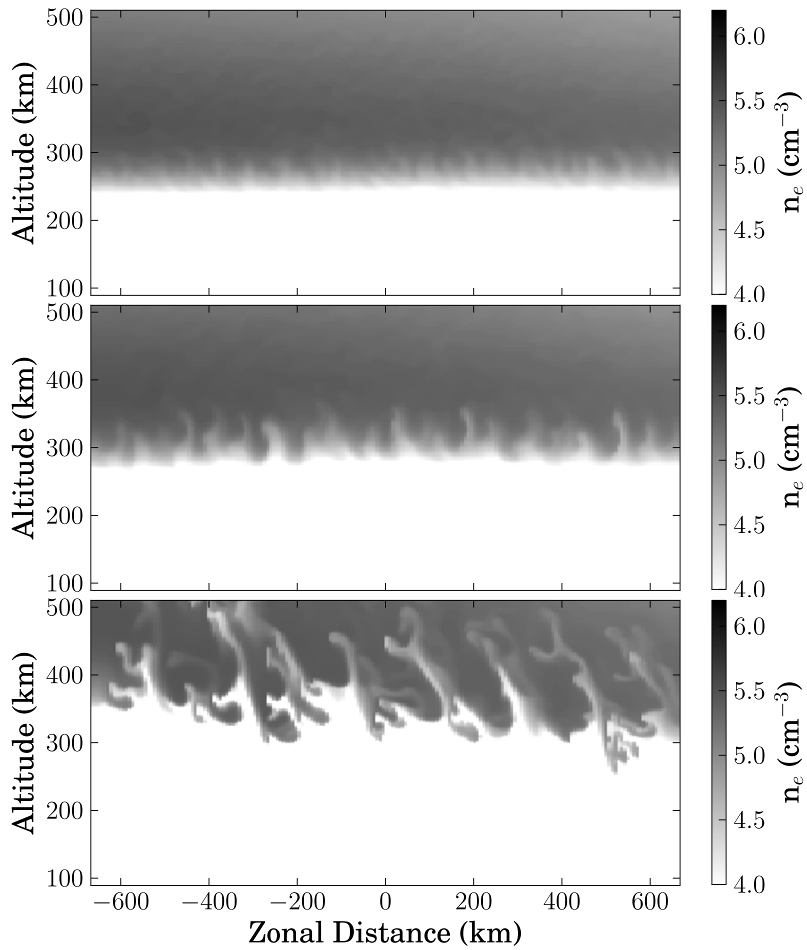

Fixed-beam radar diagnostic

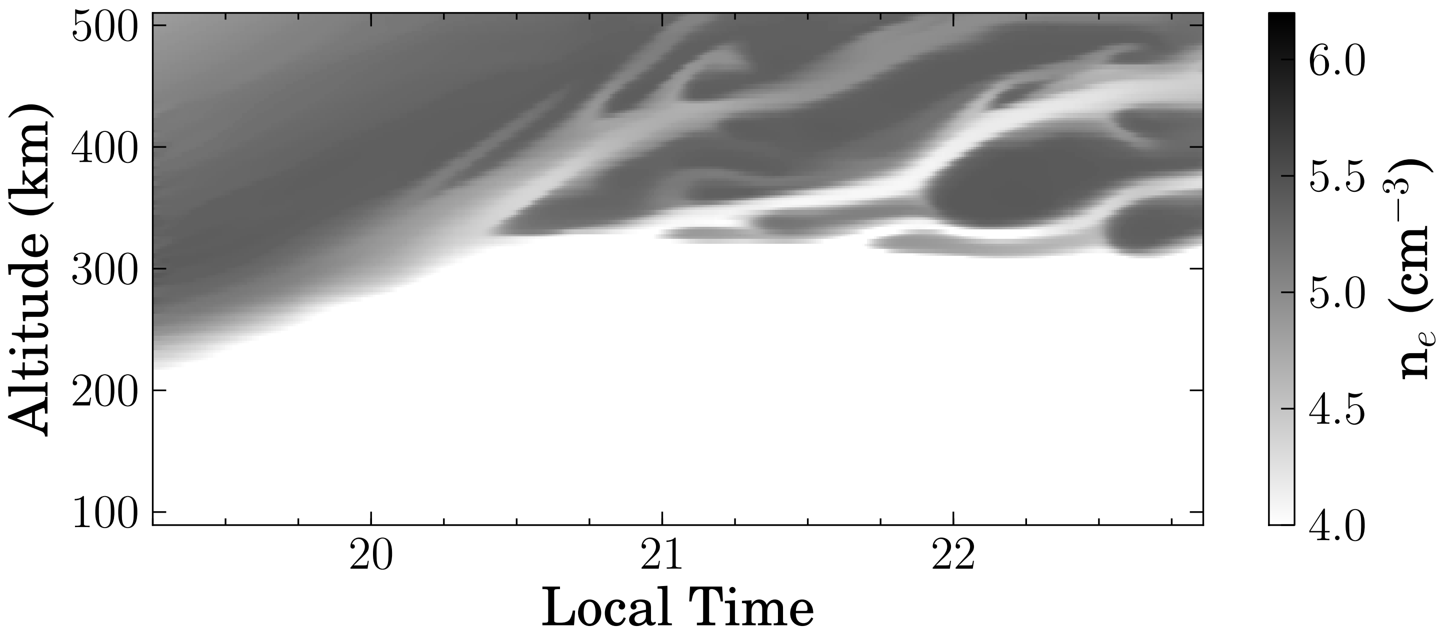

Airglow imaging diagnostic

The volume emission rate (in photons cm^{-3} s^{-1}):

$$V_{6300} = \frac{0.76\beta k_1 n_{O^+} n_{O_2}}{1 + (k_2 n_{N_2} + k_3 n_{O_2} + k_4 n_e + k_5 n_O)/A_{1D}}$$

Table: Chemistry of O(^{1}D) in the nightglow

Reaction	Rate coefficient [cm^{3}s^{-1}]*	References
$O^+ + O_2 \rightarrow O_2^+ + O$	$k_1 = 3.23 \times 10^{-12} e^{3.72/\tau_i - 1.87/\tau_i^2}$	Link and Cogger (1988
$O(^1D) + N_2 \rightarrow O(^3P) + N_2$	$k_2 = 2.0 \times 10^{-11} e^{111.8/T_n}$	
$O(^1D) + O_2 \rightarrow O(^3P) + O_2$	$k_3 = 2.9 \times 10^{-11} e^{67.5/T_n}$	
$O(^1D) + e \rightarrow O(^3P) + e$	$k_4 = 1.60 \times 10^{-12} T_e^{0.91}$	
$O(^1D) + O \rightarrow O(^3P) + O$	$k_5 = 2.55 \times 10^{-12}$	Sobral et al. (1993)

$^*\tau_i = T_i/300$

Airglow imaging diagnostic

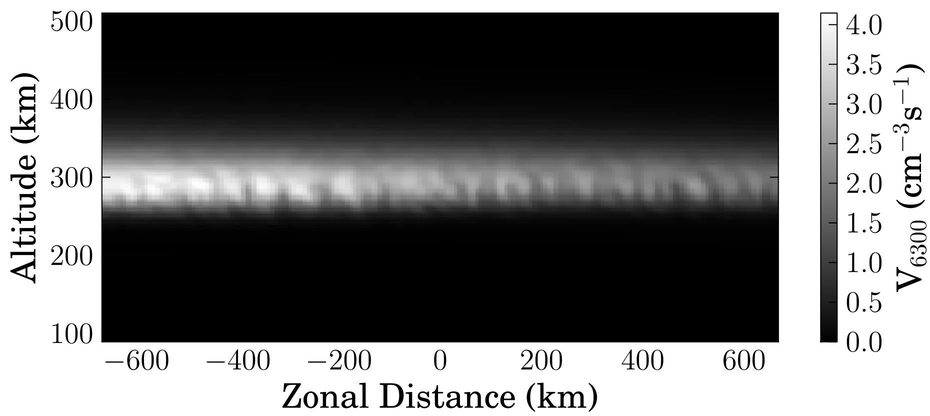

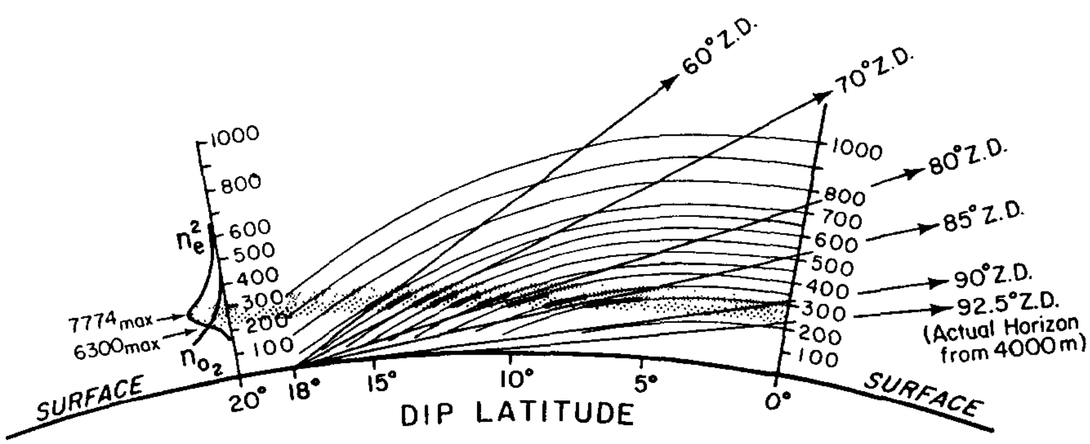

Tinsley (1982)

Airglow imaging diagnostic

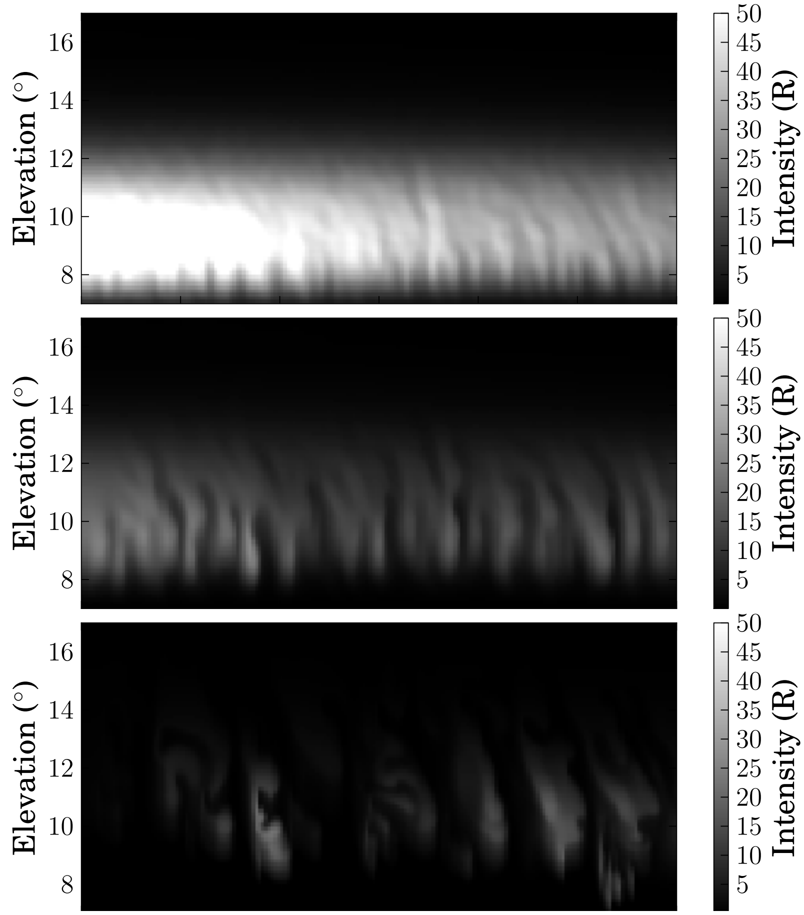

Airglow imaging diagnostic

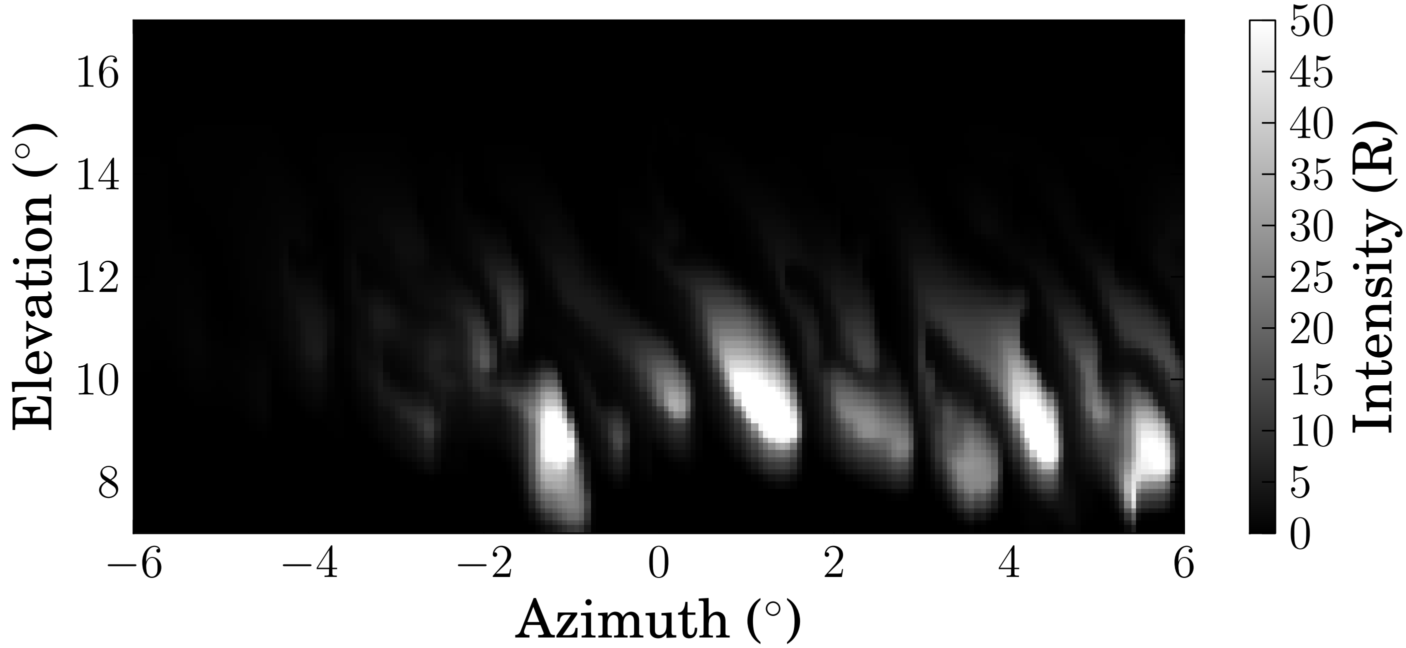

Currents and magnetic field perturbations

$$\nabla \times \mathbf{B} = \mu_0 \mathbf{J} + \mu_0 \epsilon_0 \frac{\partial \mathbf{E}}{\partial t} \rightarrow \nabla^2 \mathbf{B} = -\mu_0 \nabla \times \mathbf{J}$$

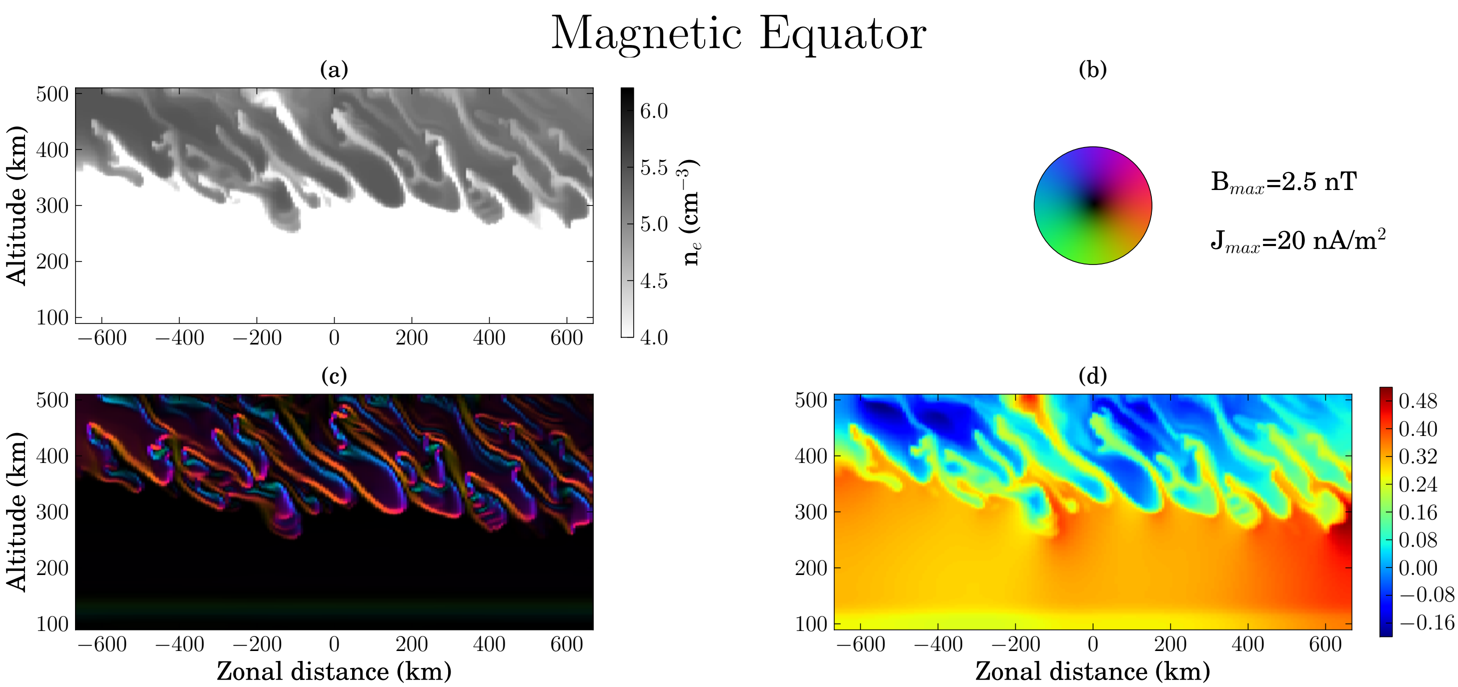

Currents and magnetic field perturbations

+4° Magnetic Lat. (North)

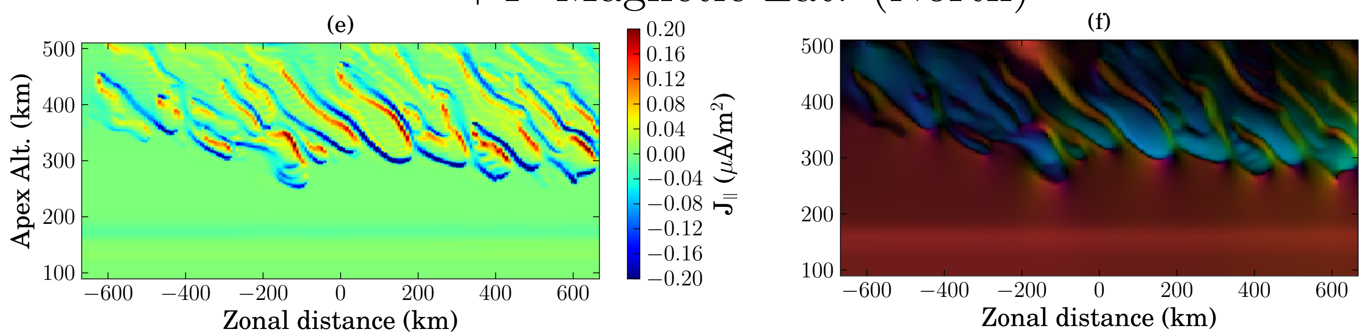

-4° Magnetic Lat. (South)

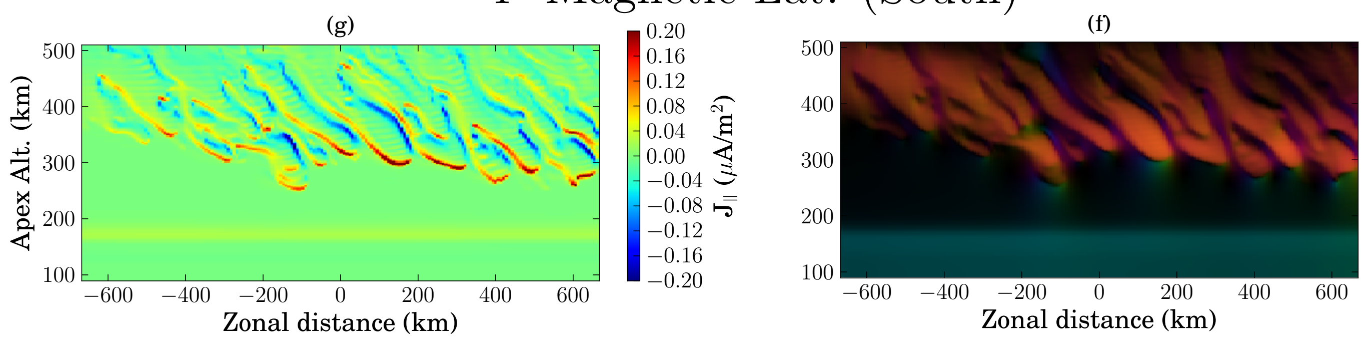

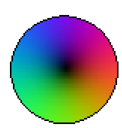

Satellite-borne magnetometer diagnostic

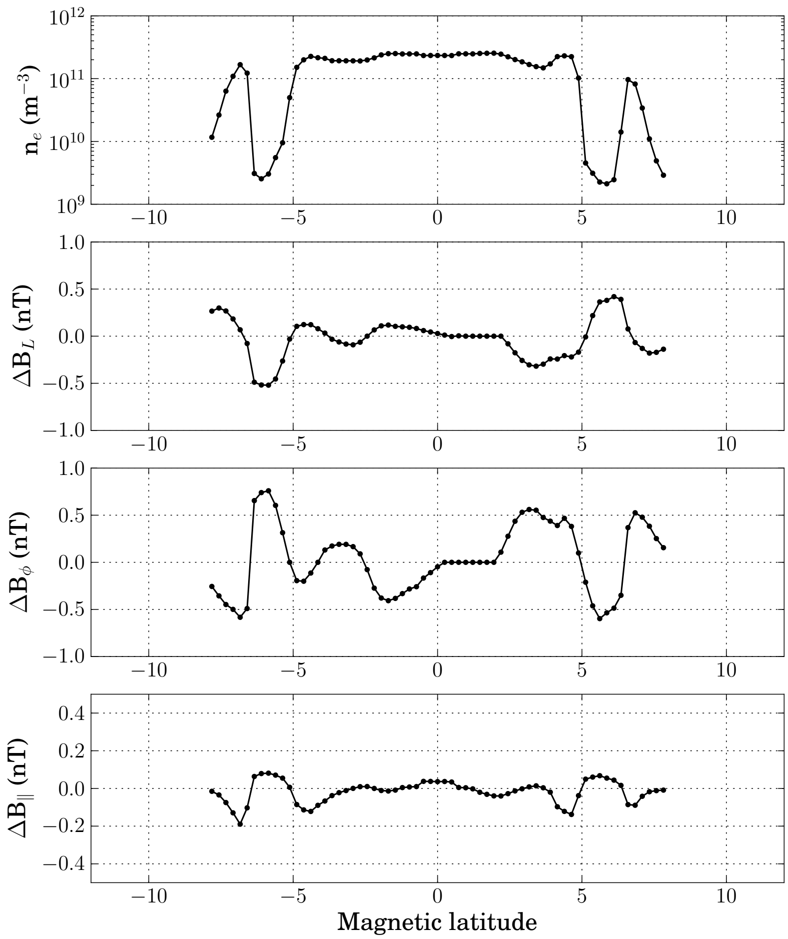

Summary

- the simulation of coherent/incoherent scatter observations showed the typical three stages of ESF evolution, from bottom-type to bottomside to topside spread *F*;
- some of the features include westward tilted ascending depletions connected to the bottomside, periodic spacing of 100-200 km in the zonal direction, bifurcation, secondary instabilities growing on the western walls of the primaries, and rates of development;
- the comparison between the simulated radar scans and airglow simulations showed that details of the plasma irregularities have been lost and waveforms appeared distorted in airglow observations;
- simulated magnetic field perturbations show good qualitative with the CHAMP measurements as derived in a statistical study by Park et al. (2009), as e.g. upward (downward) currents on their external western (eastern) edges.

THANKS!